

# 1 Homoploid Hybridization Resolves the Origin of Octoploid 2 Strawberries

3 Zhen Fan<sup>1</sup>, Aaron Liston<sup>2\*</sup>, Douglas Soltis<sup>3</sup>, Pamela Soltis<sup>3</sup>, Tia-Lynn Ashman<sup>4</sup>, Kim Hummer<sup>5</sup>,  
4 Vance M. Whitaker<sup>1\*</sup>

5 1 Horticultural Sciences Department, University of Florida, IFAS Gulf Coast Research and  
6 Education Center, Wimauma, FL, 33597, USA.

7 2 Department of Botany and Plant Pathology, Oregon State University, Corvallis, OR, 97331,  
8 USA.

9 3 Florida Museum of Natural History, University of Florida, Gainesville, FL, 32611, USA.

10 4 Department of Biological Sciences, University of Pittsburgh, Pittsburgh, PA, 15260, USA.

11 5 USDA ARS National Clonal Germplasm Repository, Corvallis, OR, 97333, USA.

12 Corresponding authors:

13 Aaron Liston: aaron.liston@oregonstate.edu

14 Vance M. Whitaker: vwhitaker@ufl.edu

15

## 16 Abstract

17 The identity of the diploid progenitors of octoploid cultivated strawberry (*Fragaria × ananassa*)  
18 has been subject to much debate. Past work identified four subgenomes and consistent  
19 evidence for *F. californica* (previously named *F. vesca* subsp. *bracteata*) and *F. iinumae* as  
20 donors for subgenomes A and B, respectively, with conflicting results for the origins of  
21 subgenomes C and D. Here, reticulate phylogeny and admixture analysis support hybridization  
22 between *F. viridis* and *F. vesca* in the ancestry of subgenome A, and between *F. nipponica* and  
23 *F. iinumae* in the ancestry of subgenome B. Using an LTR-age-distribution-based approach, we  
24 estimate that the octoploid and its intermediate hexaploid and tetraploid ancestors emerged  
25 approximately 0.8, 2, and 3 million years ago, respectively. These results provide an explanation  
26 for previous reports of *F. viridis* and *F. nipponica* as donors of the C and D subgenomes and  
27 unify conflicting hypotheses about the evolutionary origin of octoploid *Fragaria*.

## 28 Main

29 *Fragaria*, commonly known as strawberry, exhibits a range of ploidy from diploid to decaploid  
30 ( $2n = 2x - 10x = 14 - 70$ ) and occurs across the Northern Hemisphere. The octoploid cultivated  
31 strawberry (*Fragaria × ananassa*) is a vitally important fruit crop with steadily increasing  
32 consumption<sup>1</sup>. Although the cultivated strawberry has a short ~300-year history since its origins  
33 via interspecific hybridization between *Fragaria chiloensis* and *Fragaria virginiana*, these two  
34 octoploid progenitors evolved through a series of whole-genome duplication events,  
35 hybridizations, and subsequent adaptation over millions of years<sup>2</sup>.

36 Polyploidy, the condition of possessing more than two complete sets of chromosomes, has been  
37 a pivotal mechanism in the diversification and adaptation of many plant species<sup>3-5</sup>. In  
38 strawberries, polyploidy has contributed not only to increased genetic diversity but also to the

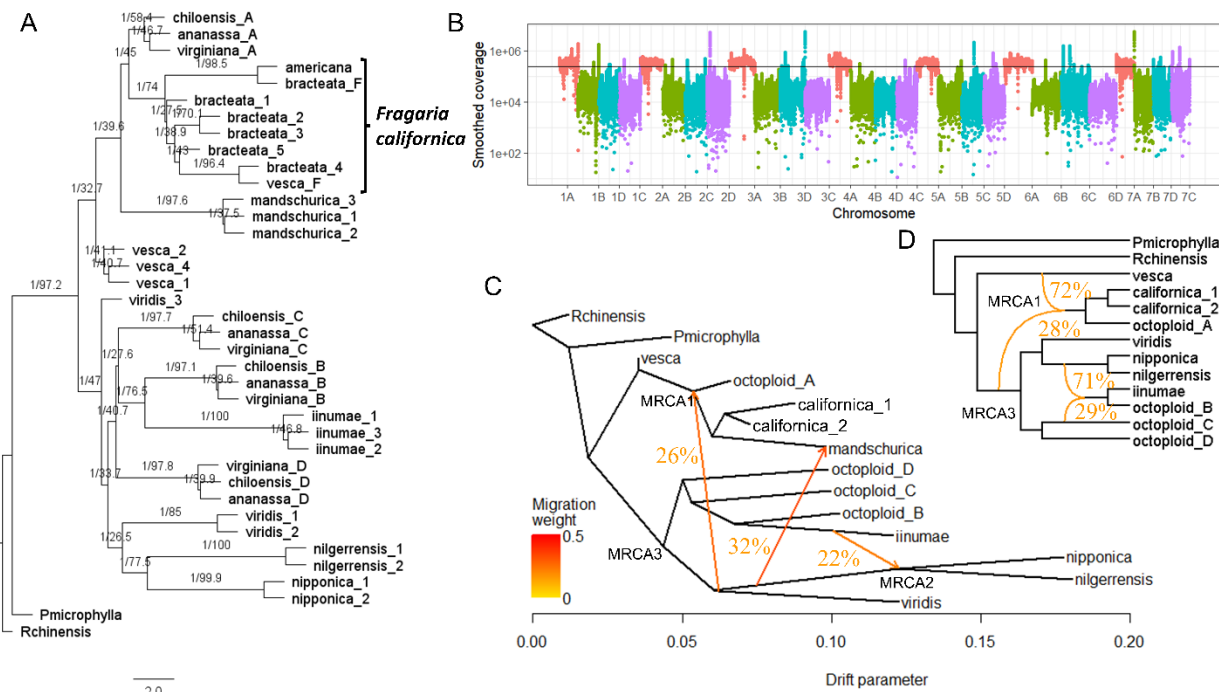
39 enhancement of desirable traits such as fruit size, biomass, and resistance to environmental  
40 stresses. Unlike some other recent polyploids which experienced recurrent polyploidization<sup>6</sup>,  
41 current phylogenetic evidence supports a single origin of wild octoploid species<sup>7</sup>. The octoploid  
42 strawberry genome has four subgenomes, A, B, C, and D, which originated from four different  
43 diploid species. There is scientific consensus that *F. vesca* subsp. *bracteata* (renamed here *F.*  
44 *californica*, see Results and Discussion) and *F. iinumae* served as the donors for subgenomes A  
45 and B, respectively, but the origins of subgenomes C and D have been debated<sup>2,8–10</sup>.  
46 Phylogenetic signal from *F. viridis* in the octoploids was first supported by sequences of low-  
47 copy genes<sup>11</sup>. Based on phylogenetic analysis of ortholog sequences from the first  
48 chromosome-scale genome assembly of octoploid strawberry, Edger et al.<sup>2</sup> proposed that *F.*  
49 *viridis* and *F. nipponica* were donors for subgenomes C and D, respectively. Others proposed  
50 that subgenomes C and D formed a sister group, sharing an ancestor with *F. iinumae*<sup>9,12–14</sup>.  
51 Based on new evidence from subgenome-specific Kmers, subgenome assignments for the C  
52 and D subgenomes have been clarified<sup>12,14,15</sup>. In this work, we follow the subgenome  
53 assignments (Table S1) used in Jin et al.<sup>12</sup>.

54 To identify the diploid donors for the two octoploid species (*F. chiloensis* and *F. virginiana*) that  
55 are the progenitors of cultivated strawberry, it is essential to survey a wide range of diploid  
56 *Fragaria* species and elucidate their phylogenetic relationships. Previous studies using both  
57 chloroplast and nuclear genomes supported two major diploid clades, designated as the  
58 Southwest China clade (*F. pentaphylla*, *F. chinensis*, *F. nubicola*, *F. daltoniana*, and *F.*  
59 *nilgerrensis*) and the *F. vesca* clade, including *F. vesca* subspecies and *F. mandshurica*<sup>16–19</sup>.  
60 Discordance in the phylogenetic position of *F. iinumae* and *F. viridis* was reported, likely due to  
61 past interspecific hybridization and incomplete lineage sorting<sup>18</sup>. In Europe, hybrids of diploid *F.*  
62 *vesca* and *F. viridis* have been occasionally observed in areas of sympatry<sup>20</sup>. Likewise, hybrids  
63 of *F. iinumae* and *F. nipponica* exist in Japan<sup>21,22</sup>. Recently, widespread hybridization across  
64 diploid *Fragaria* species was revealed; notably, PhyloNet suggested that *F. viridis* may have  
65 contributed to the hybrid origination of the lineage of *F. chinensis*, *F. nipponica*, *F. nubicola*, and  
66 *F. pentaphylla*, and/or the lineage of *F. vesca* and *F. mandshurica*<sup>18</sup>.

67 The diploid *Fragaria* that are distributed across North America were previously identified within  
68 three subspecies of *F. vesca*<sup>23</sup>, which are *bracteata*, *americana*, and *californica*. Phylogenetic  
69 analyses of plastomes<sup>19</sup> and nuclear microsatellites<sup>24,25</sup> demonstrated the distinctiveness of the  
70 North American subspecies from Eurasian *F. vesca*, but American diploid *Fragaria* has been  
71 underrepresented in phylogenetic studies of the nuclear genome. While the northwestern North  
72 American *F. vesca* subsp. *bracteata* contributed the plastid genome<sup>19</sup> to the octoploid  
73 strawberry, whether plants from the same geographic region also contributed subgenome A  
74 remains untested, due to limited sampling in previous studies. Generating whole genome  
75 sequences of American diploids will not only help resolve their relationship with *F. vesca*, but  
76 also verify their contribution to the octoploid genome. Additionally, a reticulate phylogeny  
77 approach can help us understand how homoploid hybridization among diploid species has  
78 contributed to *Fragaria* polyploids.

79 In this study, we have sought to resolve the cryptic signals from *F. viridis* and *F. nipponica* in the  
80 octoploid strawberry genome and unify conflicting hypotheses about the evolutionary path to  
81 octoploid strawberry. Additionally, using octoploid strawberry as a model, we refined a  
82 framework to date the approximate timing of polyploidization events based on the age of  
83 insertion of long terminal repeats (LTR).

84 Using whole genome sequence data, three bifurcating phylogenetic approaches (ASTRAL, ML,  
 85 and SVDQuartets) provided similar results regarding the origins of the four subgenomes for both  
 86 octoploid strawberry species (Fig 1A, Fig. S1 and S2). These analyses showed that subgenome  
 87 A is sister to a clade of North American diploids including both *F. vesca* subsp. *bracteata* and  
 88 subsp. *americana*, subgenome B is sister to *F. iinumae*, and subgenomes C and D form a clade  
 89 with subgenome B and *F. iinumae*, confirming multiple reports <sup>8,9,12</sup>. In all three trees, two *F.*  
 90 *viridis* samples, *F. nilgerrensis*, and *F. nipponica* consistently formed a monophyletic group,  
 91 sister to the clade of subgenomes B, C, D, and *F. iinumae* clade. Based on their phylogenetic  
 92 sister relationship with *F. mandshurica* determined by both genomic and plastid DNA sequence  
 93 data <sup>7</sup>, along with their distinct morphological characteristics and geographic distributions, the  
 94 North American diploids (including *F. vesca* subsp. *bracteata*, subsp. *americana*, and subsp.  
 95 *californica*) are here designated as a single species *Fragaria californica* Cham. & Schltdl.  
 96 (1827), the oldest available name. Whether infraspecific taxa are warranted will require more  
 97 intensive sampling across the broad geographic range of the newly recognized *F. californica*.  
 98 While the plastid genome <sup>19</sup> indicates a northwest North American maternal ancestry of the  
 99 octoploid strawberry, our nuclear phylogenomic results do not resolve where in North America  
 100 subgenome A originated.



111 likelihood method. *F. mandshurica* samples were removed due to its recent hybridization to  
112 reduce network complexity.

113 In polyploids, homoeologous exchanges (HEs) and homoeologous recombination (HR) can  
114 reshuffle the genetic differences among subgenomes, leading to the admixture of ancestral  
115 information within a subgenome. Edger et al.<sup>2</sup> suggested that extensive HEs from subgenome A  
116 contributed 0.5 to 28.3% of the chromosomes in the other subgenomes. However, no signals for  
117 large-scale segmental HE were revealed by subsequent Kmer analysis<sup>14</sup>. Given the proposed  
118 biased pattern of HEs from subgenome A to the other subgenomes, our analysis focused on  
119 detecting these specific signals. Although three four-taxon trees representing the relationships  
120 among the four subgenomes and *F. californica* (Fig. S3) did not reveal significant deviations  
121 from expected relationships based on genome-wide SNPs, positive f-branch values between  
122 subgenomes B and A (fbranch = 1.67%) and between subgenomes C and A (1.08%) suggested  
123 the presence of HE (Fig. S4). To identify regions that underwent HE, we used an alignment-  
124 based approach with newly generated whole genome sequences of *F. californica*. We identified  
125 42 candidate HE regions in the B, C, and D subgenomes, totaling 2.7 Mb ( $\approx$  0.34% of the  
126 genome,  $\approx$  0.46% of the B, C, and D subgenomes), which showed high mapping coverage of *F.*  
127 *californica* sequences (Fig. 1B). The higher percentage of overlap with intact TEs (10.7%)  
128 compared to the genome-wide average (7.7%) (Fig. S5) suggests the potential inclusion of  
129 transposon-derived duplicates, despite applying a minimum size selection of 20 kb. To confirm  
130 HE in these regions, ML trees constructed using concatenated SNPs were analyzed. A sister-  
131 group relationship of subgenome A or *F. californica* instead of *F. iinumae* with one of the  
132 subgenomes B, C, or D was found in 32 regions, supporting their HE assignment (Table S2). In  
133 four cases, including the largest identified HE (farr1\_chr\_2D/2C:3820000- 4200000bp),  
134 disparities in tree topologies between the two wild octoploid species (*F. chiloensis* and *F.*  
135 *virginiana*) suggest that these HE occurred after the divergence of the two octoploid species,  
136 distinguishing them from hybridization among diploids prior to octoploidization. Lastly, for the  
137 largest HE, differences in synteny between *F. chiloensis* and *F. virginiana* vs. *F. vesca*  
138 corroborate occurrence of this HE after divergence of the two octoploid species (Fig. S6). Our  
139 results validated HE occurrence during evolution of octoploid strawberry, though its scale was  
140 much smaller than previous estimates<sup>2,26</sup>. This is likely a result of using reads from the direct  
141 donor species of the A subgenome and the exclusion of transposon-derived duplications.

142 Although *F. californica* and *F. iinumae* were the only species recognized as extant diploid  
143 progenitors of the ancestral octoploid strawberry in this and multiple previous studies, elevated  
144 mapping coverage of *F. viridis* and *F. nipponica* sequences to the octoploid genome<sup>12,13</sup> and a  
145 sister relationship with octoploid orthologs in a substantial number of gene trees were often  
146 observed<sup>2,10,11</sup>. Therefore, multiple phylogenetic network approaches (Treemix, admixture graph  
147 and PhyloNet) were used to infer hybridization during the evolution of the octoploid species.  
148 Three hybridization events were determined as the optimal number in Treemix<sup>27</sup>. The inferred  
149 hybridization edges were from *F. viridis* to the MRCA (MRCA1) of subgenome A of the octoploid  
150 species, *F. californica*, and *F. mandshurica* (Migration weight = 26.1%); from the MRCA  
151 (MRCA2) of *F. nipponica* and *F. nilgerrensis* to *F. mandshurica* (32.73%); and from *F. iinumae*  
152 to MRCA2 (21.6%) (Fig. 1C). The admixture graph<sup>28</sup> estimated that introgression from *F. viridis*  
153 contributed 24% (CI: 13%-37%) to the genome of MRCA1. The other two admixture proportions  
154 were 26% (CI: 10%-38%, MRCA2 to *F. mandshurica*) and 28% (CI: 11%-96%, *F. iinumae* to  
155 MRCA2), respectively (Fig. S7). PhyloNet results corroborated that MRCA1 was a hybrid, but its  
156 second parental species was assigned to MRCA3 (Fig. 1D, 28%), which is the MRCA of all

157 sampled diploid species except the *F. vesca* clade. In contrast, the Phylonet analysis suggests  
158 that the ancestor of *F. iinumae* and subgenome B could be a hybrid or that *F. iinumae* has  
159 introgressed into both *F. nipponica* and the diploid donor of subgenome C.

160 Therefore, the phylogenetic sister relationship of octoploid and *F. viridis* orthologs and higher  
161 mapping rates of *F. viridis* to the octoploid genomes appear to result from its introgression into  
162 the ancestor of subgenome A prior to octoploidization. On the other hand, the close relationship  
163 of *F. nipponica* and octoploids in gene trees is likely due to its hybridization with *F. iinumae*.  
164 These results reconcile the conflicting phylogenetic hypotheses for the origins of the octoploid  
165 subgenomes <sup>2,9,10</sup>.

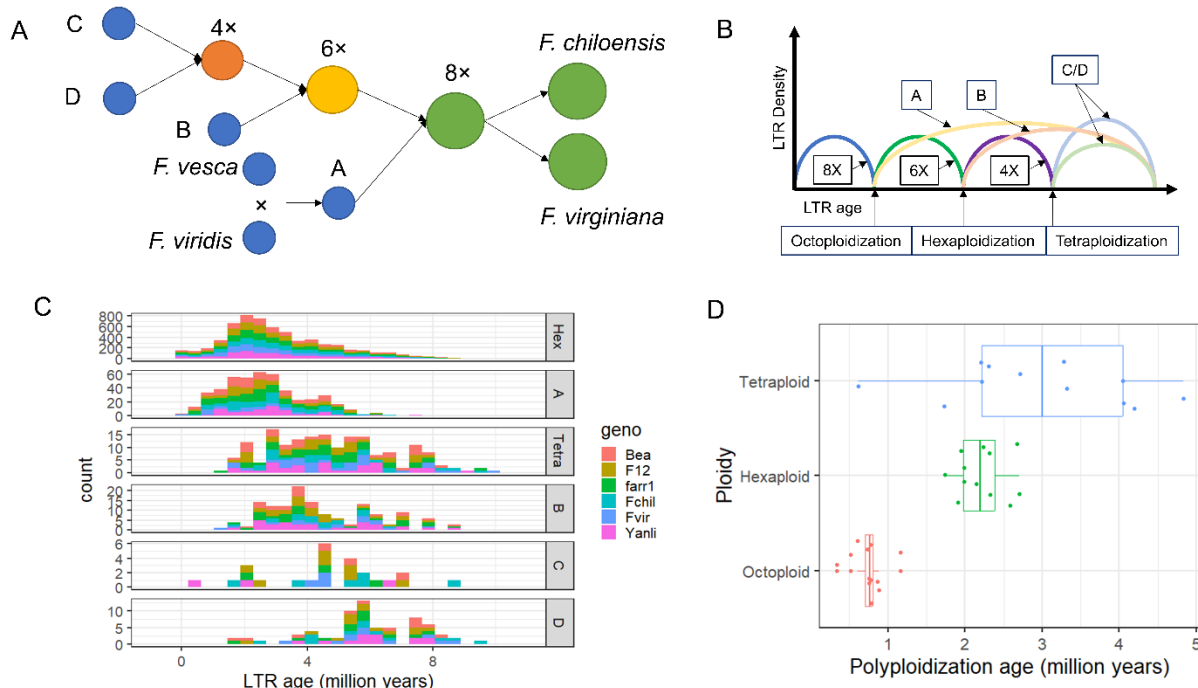
166 Both Ks-based and phylogeny-based age estimation <sup>29</sup> are unsuitable for octoploid strawberry  
167 due to its recent genome duplication and the presumed extinction of the C and D diploid donors  
168 <sup>8,30</sup>. Recently, LTR age estimation has been used to provide a range of values for the age of  
169 polyploids <sup>31</sup>. LTR movement occurs continuously, acting like timestamp embedded in the  
170 genome, and specific LTRs are active at different times and in even closely related species <sup>32,33</sup>.  
171 Therefore, the timing of LTR insertions that uniquely distributed in individual subgenomes  
172 provided a way to date polyploidization events. For octoploid strawberry, Session & Rokhsar <sup>14</sup>  
173 estimated that hexaploidization occurred around 3 million years ago (MYA) based on the peak in  
174 age distribution for common LTRs shared by the B, C, and D subgenomes. Our approach seeks  
175 to refine these estimates by providing estimates and confidence intervals (CI) for the ages of the  
176 octoploid, intermediate hexaploid and tetraploid based on LTR age, as explained below.

177 All subgenome donors (A, B, C, D) of octoploid strawberry share a common ancestor. Once  
178 they diverged, each diploid species began accumulating species-specific LTRs in their genomes  
179 until they hybridized into a polyploid species. The polyploidizations that formed octoploid  
180 strawberry occurred in a specific sequence: tetraploid (C and D subgenomes), hexaploid (B, C  
181 and D subgenomes), and then octoploid (Fig. 2A) <sup>14</sup>. The timing of the hybridization event  
182 between the C and D donors can be dated using the insertion time of the youngest C- and D-  
183 specific LTRs (Fig. 2B). After this hybridization event, in the tetraploid ancestor, LTR movement  
184 was random, allowing the same LTR to insert into either the C or D subgenome. As a result, the  
185 C and D subgenomes share LTRs that were active in the tetraploid ancestor; the youngest LTRs  
186 in the intermediate tetraploid and subgenome B donor can be used to determine the age of  
187 hexaploid formation (Fig. 2B). The same process applies when the tetraploid ancestor  
188 hybridized with the B subgenome donor, at which point newer LTRs began to be shared among  
189 the B, C, and D subgenomes. Using 5% quantiles of these LTR age distributions and six  
190 independent genome assemblies of octoploid species, we could determine the age and its  
191 confidence interval (CI) for each polyploidization event. The LTR age distributions confirmed the  
192 order of polyploidization, with the LTRs specific to subgenomes C and D showing the oldest  
193 distribution, whereas subgenome A and the intermediate hexaploid showed the youngest (Fig.  
194 2C, Supplementary Data1). The LTR-based approach estimated that tetraploidization between  
195 the C and D subgenome donors occurred approximately 3.0 MYA (CI = [4.5, 1.2]),  
196 hexaploidization with the B subgenome donor at roughly 2.2 MYA (CI = [2.7, 1.8]), and  
197 octoploidization with the A subgenome donor at 0.8 MYA (CI = [1.0, 0.4]) (Fig. 2D). Because the  
198 LTR approach is not influenced by the absence of diploid donors and hybridization prior to  
199 polyploidization, its estimates were lower than those from phylogeny-based approaches (Table  
200 1). Our age estimation for the formation of the octoploid is close to the estimate based on a  
201 calibrated tree inferred from plastid DNA sequences (1MYA) <sup>7</sup>. The CIs for both hexaploid and

202 octoploid formation were less than 1 MYA. However, for the most ancient polyploidization, the  
203 retention of intact subgenome-specific TEs was low, especially for subgenome C, resulting in a  
204 wide CI for tetraploid formation.

205 These age estimates are consistent with the earliest fossil records of *Fragaria* from the Late  
206 Pliocene (3.6-2.6 Ma) of the Canadian Arctic and Yunnan, China. The Canadian record was  
207 based on a single well-preserved achene, but no image or specimen is available<sup>20,34</sup>. The  
208 Chinese record is based on 19 well-preserved achenes that are vouchered and photographed<sup>35</sup>. A Miocene report of *Fragaria* is considered unreliable, as it compares the fruiting structure to  
209 both *Fragaria vesca* and *Potentilla indica* (as *Fragaria indica*)<sup>36</sup>.

211 It has been hypothesized that these sequential allopolyploidization events 3.0-0.8 MYA leading  
212 to the origin of octoploid *Fragaria* occurred in Beringia<sup>30</sup>. During this time frame, Beringia is  
213 hypothesized to have been characterized by mixed conifer forests with a diverse herbaceous  
214 understory<sup>37</sup>, appropriate habitat for *Fragaria*. Whether the homoploid hybridization events  
215 inferred here also occurred in Beringia is unknown. Environmental DNA (eDNA) has  
216 documented over 100 different plant genera from a 2-million-year-old ecosystem in northern  
217 Greenland<sup>38</sup>; eDNA studies in the former Beringia could potentially provide physical evidence  
218 bearing on the evolutionary history proposed here.



219  
220 Figure 2. Dating the approximate timing of polyploidization in the formation of octoploid  
221 strawberry. (A) Schematics of evolutionary path to octoploid *Fragaria*. (B) Theoretical LTR age  
222 distributions in subgenome donors (A, B, C, and D) and intermediate polyploid ancestors  
223 (Intermediate tetraploid: 4X, Intermediate tetraploid: 6X, octoploid: 8X). (C) Cumulative LTR age  
224 distributions in diploid subgenome donors (A, B, C and D) and intermediate hexaploid (Hex) and  
225 tetraploid (Tetra) ancestors across six genomes. Bea, F12, farr1 and Yanili are genome  
226 assemblies of *F. × ananassa* accessions. Fchil and Fvir are genomes of *F. chiloensis* and *F.*  
227 *virginiana*, respectively. (D) Boxplots of age estimates for polyploidization events. Each dot

228 represents one estimate based on one LTR distribution of one genome assembly. A total of 12  
229 data points is used to date each polyploidization event.

230

231 Table 1. Phylogenetic dating of octoploid and intermediate polyploid ancestors of octoploid  
232 strawberry.

Formation	LTR age-based approach	Phylogeny-based approach					
		Filtered single-copy orthologs <sup>a</sup>			All single-copy orthologs		
		R8s <sup>b</sup>	LSD2	RelTime	R8s	LSD2	RelTime
Octoploid	0.8	2.74	1.91	1.44	3.33	2.23	2.23
	(1.0, 0.4) <sup>c</sup>	(2.80, 2.67)	(2.61, 1.51)		(3.42, 3.22)	(2.91, 1.85)	1.73
Hexaploid	2.2	6.74	5.10	3.30	6.27	5.29	5.29
	(2.7, 1.8)	(6.87, 6.60)	(6.33, 4.02)		(6.39, 6.18)	(6.93, 4.20)	3.41
Tetraploid	3.0	7.91	6.24	4.06	7.18	6.32	6.32
	(4.5, 1.2)	(8.05, 7.75)	(7.97, 5.18)		(7.27, 7.08)	(8.23, 5.19)	4.10

a Orthologs which showed potential admixture signals based on four-taxon trees were removed.

b R8s, LSD2, and RelTime are three popular methods for dating evolutionary divergences.

c Confidence intervals are given.

233

234 In summary, based on admixture analyses and reticulate phylogeny, we propose that homoploid  
235 hybridization between *F. viridis* and *F. vesca* led to the formation of the North American *F.*  
236 *californica* and subgenome A of octoploid strawberry. Hybridization among *F. iinumae*, *F.*  
237 *nipponica*, and possibly the donor of subgenome C might have resulted in the sister relationship  
238 of *F. nipponica* and octoploid species in gene trees. Homoeologous exchange contributed to  
239 genome reshuffling but only on a small scale. These findings resolve conflicting hypotheses  
240 about the evolutionary origin of octoploid strawberry and will guide efforts to enhance genetic  
241 diversity in *F. × ananassa* from diploid species through interspecific hybrid and horizontal gene  
242 transfer. Our framework for dating polyploidization events using the 5% quantiles of LTR age  
243 distributions in intermediate polyploids and diploid donors produced estimated ages of octoploid,  
244 intermediate hexaploid, and tetraploid formation in the octoploid strawberry as 0.8, 2, and 3  
245 MYA, respectively. This approach, which does not require sequences from extant ancestral  
246 diploid species, provides a valuable addition to existing methods for dating polyploidization  
247 events when subgenome donor species are unavailable.

## 248 Materials and methods

### 249 Sample collection and sequencing

250 Freeze-dried leaves of ten diploid *Fragaria* samples, including five *F. vesca* subsp. *bracteata*  
251 and one *F. vesca* subsp. *americana* samples (renamed as *F. californica* based on results), were  
252 used for CTAB DNA extraction. The geographic location and taxon designation of each sample  
253 are provided in a supplementary table (Table S3), and voucher specimens are deposited in the  
254 Oregon State University Herbarium (OSC). DNA was sent to Novogene Corporation Inc.,  
255 Sacramento, CA, USA, for whole genome sequencing (WGS). Paired-end (2x150 bp) libraries  
256 were constructed and sequenced on Illumina HiSeq X Ten platform. Short reads of 16 additional  
257 diploid *Fragaria* samples and two outgroup species (*Potentilla microphylla* and *Rosa chinensis*)  
258 were obtained from six previous studies <sup>2,17,18,39-41</sup>. Assemblies for each subgenome in *F. ×*

259 *ananassa*<sup>42</sup>, *F. chiloensis* and *F. virginiana*<sup>12</sup> were extracted from the whole genome assemblies  
260 based on the most recent subgenome assignment<sup>12</sup>. Simulated 2x150 bp pair-end short reads  
261 for them were generated using ART V20160605<sup>43</sup>. Variant calling follows our previous work<sup>44</sup>.  
262 Briefly, reads were aligned to a chromosome-scale *F. vesca* genome assembly V6.0<sup>45</sup> using  
263 SNAP V2.0.3. SNPs and indels were called and filtered using GATK V4.4.0<sup>46</sup>.

#### 264 Species trees

265 A total of 16,114,631 SNPs and 40 terminal nodes (Table S3) including all *Fragaria* species  
266 related to origins of the octoploid species were used to reconstruct the phylogeny of *Fragaria*.  
267 Three approaches were applied: (1) SNPs were grouped into 1611 windows with 10,000  
268 variants in each. A maximum likelihood (ML) tree was constructed for each window using IQ-  
269 TREE V2.3<sup>47</sup>. ASTRAL V5.15<sup>48</sup> was used with default settings to construct a species tree with  
270 these 1611 trees as input; (2) an SVDQuartets<sup>49</sup> tree was built using the same 1611 partitions  
271 with paup V4.0; (3) a concatenated tree was inferred with all SNPs using IQ-TREE. Two  
272 previously identified *F. californica* samples (bracteata\_E1 and bracteata\_E2) were found to be  
273 octoploid samples based on uniform read-coverage distributions across four subgenomes and  
274 were thus removed from the following analyses.

#### 275 Admixture analyses and homoeologous exchange identification

276 To investigate percentages of genomic admixture, Fbranch values were obtained using Dsuite  
277 V0.4<sup>50</sup>. To identify genomic regions of HE, WGS of five *F. californica* samples were aligned to  
278 the octoploid genome<sup>42</sup>. Read coverage for every 10-kb window was obtained using the bedcov  
279 function in samtools V1.19<sup>51</sup>. Median values across samples were smoothed using the SS  
280 function (m=1, spar = 0.05) in R npreg library<sup>52</sup>. The 20% quantile of read coverage within  
281 subgenome A was used as the cutoff to identify HE regions in other subgenomes. Adjacent  
282 regions with a gap of less than 30 kb were merged. Potential HE regions smaller than 20 kb  
283 were pruned to remove signals of recent transposon insertions. Syntenic regions in the *F. vesca*  
284 genome V6.0 were inferred using CoGe SynMap (<https://genomevolution.org/coge/>). Syntenic  
285 regions were identified for 39 of 42 regions in the *F. vesca* genome<sup>45</sup>. A ML tree was inferred for  
286 each individual HE region. The topology of each tree was manually examined to validate HE.

#### 287 Reticulate networks

288 The first reticulate tree was built using TreeMix V1.12<sup>53</sup> for 10 species and four subgenomes of  
289 *F. virginiana* and *F. chiloensis*. Two or three samples of each taxon were used (Table S4). The  
290 optimal number of reticulate edges was determined using OptM<sup>27</sup>. An admixture graph<sup>28</sup> was  
291 built using Admixtools2, starting with the best TreeMix tree topology. Automated searches for  
292 better topologies with higher likelihoods did not yield improved networks. Genomic admixture  
293 percentages for the migration edges were calculated using f2 values. The third species network  
294 was constructed using Phylonet<sup>54</sup>, with the same samples and taxa as the TreeMix input,  
295 except that the *F. mandshurica* samples were removed to reduce model complexity. Maximum  
296 pseudo-likelihood networks were built with one to four reticulation nodes over 100 rounds of  
297 searching using 1611 10K-variant window trees. The network with two reticulate nodes showed  
298 a 5% improvement in likelihood over the network with one node, while the improvement dropped  
299 to 1% for three reticulate nodes (Table S5). Thus, two reticulate nodes were chosen as the best  
300 fit, consistent with the TreeMix results after the exclusion of the recent hybrid *F. mandshurica*.  
301 In a different run, a different network achieved a similar likelihood (log likelihood = -2022481) as  
302 our best network but identified MRCA3 as the hybrid of MRCA1 (Fig. 1). Given the large  
303 diversity of diploid *Fragaria* species in Asia, the older estimated age of MRCA3 compared to

304 MRCA1 (Qiao et al., 2021), and the challenges in determining the direction of hybridization<sup>55</sup>,  
305 the network shown in Figure 1D appears more plausible.

### 306 **Dating of polyploidization events**

307 High-quality genome assemblies of one *F. chiloensis*, one *F. virginiana*<sup>12</sup>, and four *F. ×*  
308 *ananassa* haplotypes<sup>42,56,57</sup> were downloaded from GDR (<https://www.rosaceae.org/>). Each  
309 assembly was separated into four subgenome-specific assemblies. Repetitive 15-mers were  
310 counted using KMC V3.2<sup>58</sup> and then filtered with minimum frequency of 100. To obtain  
311 repetitive 15-mers specific to the intermediate tetraploid and hexaploid *Fragaria*, repetitive 15-  
312 mer sets for subgenomes C and D and subgenomes B, C, and D were first intersected,  
313 respectively. Then all 15-mers of subgenome A and B, and subgenome A were removed from  
314 tetraploid and hexaploid repetitive 15-mer sets, respectively. The diploid donor-specific 15-mers  
315 were obtained by removing all 15-mers of other subgenomes from each of the subgenomic  
316 repetitive 15-mers sets. The 15-mer sets were aligned to their own octoploid genome using  
317 bowtie<sup>59</sup> with parameters (-S -v 0). Intact TEs and their insertion time for each haplotype  
318 assembly were identified and computed using EDTA V2.1<sup>60</sup>. The rate of nucleotide substitution  
319 was set to  $0.7 \times 10^{-8}$  sub/year according to previous calibration adjusted for the time of  
320 *Fragaria* MRCA at 8 MYA<sup>14</sup>. Intact LTRs overlapping with each of the 15-mer sets were  
321 extracted. A minimum coverage of 1% of the LTR and two overlapping 15-mers were used to  
322 filter the overlapping LTRs. 5% quantiles were obtained for each 15-mer set. To date polyploids  
323 based on phylogenetic trees, an ASTRAL tree was built based on 1307 single-copy orthologs.  
324 The orthologs were identified in ten diploid assemblies and four subgenomes in both *F.*  
325 *chiloensis* and *F. virginiana* using OrthoFinder<sup>61</sup>. MAFFT<sup>62</sup> and IQ-Tree were used to align  
326 orthologs and infer gene trees. Three popular phylogenetic dating methods, R8s<sup>63</sup>, LSD2<sup>64</sup>  
327 and RelTime<sup>65</sup> were applied. Two fossils were used for calibration: The *Rosa* fossil calibration is  
328 based on an Early Eocene (55.8 - 48.6 Ma) mold/impression fossil from Idaho, U.S.A.<sup>66</sup>,  
329 confirmed by Bruce Tiffney (paleobiodb.org). The *Potentilla* fossil calibration is based on an  
330 Oligocene (33.9-23.0 Ma) mold/impression fossil from Montana, U.S.A.<sup>67</sup> confirmed by Hallie  
331 Sims (paleobiodb.org). PL and TN method with 100 bootstrap datasets was applied in R8s to  
332 obtain confidence interval for divergence time. *Potentilla microphylla* (23 MYA) fossil was  
333 applied as fixed age in R8s. The substitution model “JTT+F+I+R8” was set in LSD2. To reduce  
334 the effect of *F. viridis* introgression into *F. vesca* and the absence of *F. californica* genome,  
335 dating was also inferred using non-admixed gene trees filtered by a four-taxon tree (*P.*  
336 *microphylla*, *F. viridis*, (*F. vesca*, *F. virginiana* subgenome A)). ASTRAL was used to build a tree  
337 from this non-admixed gene set as the input for dating.

## 338 **Data Availability**

339 All codes are deposited in Github (<https://github.com/zhen0506/Strawberry-Homoploid->  
340 Hybridization-). Supplementary data include species trees, raw input and output of phylogenetic  
341 dating software and SNP database is available in Zenodo (10.5281/zenodo.13513299). Raw  
342 sequencing data is available in NCBI (PRJNA1153529).

343

## 344 **References:**

345 1. Yeh, D. A., Kramer, J., Calvin, L. & Weber, C. E. The changing landscape of U.S.  
346 strawberry and blueberry markets. (2023) doi:10.32747/2023.8134359.ERS.

347 2. Edger, P. P. *et al.* Origin and evolution of the octoploid strawberry genome. *Nat*  
348 *Genet* 51, 541–547 (2019).

349 3. Soltis, D. E. & Soltis, P. S. Polyploidy: recurrent formation and genome evolution.  
350 *Trends Ecol Evol* 14, 348–352 (1999).

351 4. van de Peer, Y., Ashman, T. L., Soltis, P. S. & Soltis, D. E. Polyploidy: an  
352 evolutionary and ecological force in stressful times. *Plant Cell* 33, 11–26 (2021).

353 5. Wendel, J. F. The wondrous cycles of polyploidy in plants. *Am J Bot* 102, 1753–  
354 1756 (2015).

355 6. Leitch, A. R. *et al.* Recent and recurrent polyploidy in *Tragopogon* (Asteraceae):  
356 cytogenetic, genomic and genetic comparisons. *Biological Journal of the Linnean*  
357 *Society* 82, 485–501 (2004).

358 7. Dillenberger, M. S., Wei, N., Tennessen, J. A., Ashman, T. L. & Liston, A. Plastid  
359 genomes reveal recurrent formation of allopolyploid *Fragaria*. *Am J Bot* 105, 862–  
360 874 (2018).

361 8. Tennessen, J. A., Govindarajulu, R., Ashman, T. L. & Liston, A. Evolutionary  
362 Origins and Dynamics of Octoploid Strawberry Subgenomes Revealed by Dense  
363 Targeted Capture Linkage Maps. *Genome Biol Evol* 6, 3295–3313 (2014).

364 9. Liston, A. *et al.* Revisiting the origin of octoploid strawberry. *Nature Genetics* 2019  
365 52:1 52, 2–4 (2020).

366 10. Edger, P. P. *et al.* Reply to: Revisiting the origin of octoploid strawberry. *Nat Genet*  
367 52, 5–7 (2020).

368 11. Yang, Y. & Davis, T. M. A New Perspective on Polyploid *Fragaria* (Strawberry)  
369 Genome Composition Based on Large-Scale, Multi-Locus Phylogenetic Analysis.  
370 *Genome Biol Evol* 9, 3433–3448 (2017).

371 12. Jin, X. *et al.* Haplotype-resolved genomes of wild octoploid progenitors illuminate  
372 genomic diversifications from wild relatives to cultivated strawberry. *Nature Plants*  
373 2023 1–15 (2023) doi:10.1038/s41477-023-01473-2.

374 13. Feng, C. *et al.* Tracing the Diploid Ancestry of the Cultivated Octoploid Strawberry.  
375 *Mol Biol Evol* 38, 478–485 (2021).

376 14. Session, A. M. & Rokhsar, D. S. Transposon signatures of allopolyploid genome  
377 evolution. *Nature Communications* 2023 14:1 14, 1–14 (2023).

378 15. Jia, K. H. *et al.* SubPhaser: a robust allopolyploid subgenome phasing method  
379 based on subgenome-specific k-mers. *New Phytologist* 235, 801–809 (2022).

380 16. Qiao, Q. *et al.* Comparative transcriptomics of strawberries (*Fragaria* spp.)  
381 provides insights into evolutionary patterns. *Front Plant Sci* 7, 1839 (2016).

382 17. Qiao, Q. *et al.* Evolutionary history and pan-genome dynamics of strawberry  
383 (*Fragaria* spp.). *Proc Natl Acad Sci U S A* 118, 2105431118 (2021).

384 18. Feng, C., Wang, J., Liston, A. & Kang, M. Recombination variation shapes  
385 phylogeny and introgression in wild diploid strawberries. *Mol Biol Evol* (2023)  
386 doi:10.1093/MOLBEV/MSAD049.

387 19. Njuguna, W., Liston, A., Cronn, R., Ashman, T. L. & Bassil, N. Insights into  
388 phylogeny, sex function and age of *Fragaria* based on whole chloroplast genome  
389 sequencing. *Mol Phylogenet Evol* 66, 17–29 (2013).

390 20. Liston, A., Cronn, R. & Ashman, T. L. *Fragaria*: a genus with deep historical roots  
391 and ripe for evolutionary and ecological insights. *Am J Bot* 101, 1686–1699 (2014).

392 21. Hummer, K. E., Nathewet, P. & Davis, T. Unusual polyploidy in wild strawberry  
393 species. *Acta Hortic* 1049, 113–123 (2014).

394 22. Hummer, K. E., Postman, J. D., Bassil, N. & Nathewet, P. Chromosome numbers  
395 and flow cytometry of strawberry wild relatives. *Acta Hortic* 948, 169–174 (2012).

396 23. Staudt, G. *Systematics and Geographic Distribution of the American Strawberry  
397 Species: Taxonomic Studies in the Genus Fragaria (Rosaceae:Potentilleae)*.  
398 University of California Press, Berkeley, CA. (1999).

399 24. Hilmarsson, H. S. *et al.* Population genetic analysis of a global collection of  
400 *Fragaria vesca* using microsatellite markers. *PLoS One* 12, e0183384 (2017).

401 25. Stanley, L., Forrester, N. J., Govindarajulu, R., Liston, A. & Ashman, T. L.  
402 Geographic patterns of genetic variation in three genomes of North American  
403 diploid strawberries with special reference to *Fragaria vesca* subsp. *bracteata*.  
404 *Botany* 93, 573–588 (2015).

405 26. Liston, A. & Ashman, T. L. The origin and subgenome dynamics of the octoploid  
406 strawberries. *Acta Hortic* 1309, 107–118 (2021).

407 27. Fitak, R. R. OptM: estimating the optimal number of migration edges on population  
408 trees using Treemix. *Biol Methods Protoc* 6, (2021).

409 28. Maier, R. *et al.* On the limits of fitting complex models of population history to f-  
410 statistics. *Elife* 12, (2023).

411 29. *Polypliody*. vol. 2545 (Springer US, New York, NY, 2023).

412 30. Liston, A. On the origin of strawberries. *Nature Plants* 2023 9:8 9, 1176–1177  
413 (2023).

414 31. Lovell, J. T. *et al.* Genomic mechanisms of climate adaptation in polyploid  
415 bioenergy switchgrass. *Nature* 2021 590:7846 590, 438–444 (2021).

416 32. Ma, J., Devos, K. M. & Bennetzen, J. L. Analyses of LTR-retrotransposon  
417 structures reveal recent and rapid genomic DNA loss in rice. *Genome Res* 14,  
418 860–869 (2004).

419 33. Dangel, A. W., Baker, B. J., Mendoza, A. R. & Yu, C. Y. Complement component  
420 C4 gene intron 9 as a phylogenetic marker for primates: long terminal repeats of  
421 the endogenous retrovirus ERV-K(C4) are a molecular clock of evolution.  
422 *Immunogenetics* 42, 41–52 (1995).

423 34. Matthews, J. V *et al.* Late Tertiary Plant Macrofossils from Localities in  
424 Arctic/Subarctic North America: A Review of the Data. *Arctic* 43, 364–392 (1990).

425 35. Huang, Y. J., Zhu, H., Momohara, A., Jia, L. B. & Zhou, Z. K. Fruit fossils of  
426 Rosoideae (Rosaceae) from the late Pliocene of northwestern Yunnan, Southwest  
427 China. *J Syst Evol* 57, 180–189 (2019).

428 36. Szafer, W. 1886-1970. *Mioceńska Flora Ze Starych Gliwic Na Śląsku. : Miocene*  
429 *Flora from Stare Gliwice in Upper Silesia.* (Wydawn. geologiczne, 1961).

430 37. Fletcher, T. L., Telka, A., Rybczynski, N. & Matthews, J. V. Neogene and early  
431 pleistocene flora from alaska, usa and arctic/subarctic Canada: New data,  
432 intercontinental comparisons and correlations. *Palaeontologia Electronica* 24,  
433 (2021).

434 38. Kjær, K. H. *et al.* A 2-million-year-old ecosystem in Greenland uncovered by  
435 environmental DNA. *Nature* 2022 612:7939 612, 283–291 (2022).

436 39. Fan, W. *et al.* Fragaria mitogenomes evolve rapidly in structure but slowly in  
437 sequence and incur frequent multinucleotide mutations mediated by  
438 microinversions. *New Phytologist* 236, 745–759 (2022).

439 40. Buti, M. *et al.* The genome sequence and transcriptome of Potentilla micrantha and  
440 their comparison to Fragaria vesca (the woodland strawberry). *Gigascience* 7, 1–  
441 14 (2018).

442 41. Raymond, O. *et al.* The Rosa genome provides new insights into the domestication  
443 of modern roses. *Nature Genetics* 2018 50:6 50, 772–777 (2018).

444 42. Hardigan, M. A. *et al.* Blueprint for Phasing and Assembling the Genomes of  
445 Heterozygous Polyploids: Application to the Octoploid Genome of Strawberry.  
446 *BioRxiv* 467115 (2021) doi:<https://doi.org/10.1101/2021.11.03.467115>.

447 43. Huang, W., Li, L., Myers, J. R. & Marth, G. T. ART: a next-generation sequencing  
448 read simulator. *Bioinformatics* 28, 593–594 (2012).

449 44. Fan, Z. & Whitaker, V. M. Genomic signatures of strawberry domestication and  
450 diversification. *Plant Cell* 36, 1622–1636 (2024).

451 45. Zhou, Y. *et al.* The telomere-to-telomere genome of Fragaria vesca reveals the  
452 genomic evolution of Fragaria and the origin of cultivated octoploid strawberry.  
453 *Hortic Res* 10, (2023).

454 46. Van der Auwera, G., O'Connor, B. & Safari. *Genomics in the Cloud: Using Docker,*  
455 *GATK, and WDL in Terra.* O'Reilly Media (books.google.com, 2020).

456 47. Minh, B. Q. *et al.* IQ-TREE 2: New Models and Efficient Methods for Phylogenetic  
457 Inference in the Genomic Era. *Mol Biol Evol* 37, 1530–1534 (2020).

458 48. Zhang, C., Rabiee, M., Sayyari, E. & Mirarab, S. ASTRAL-III: Polynomial time  
459 species tree reconstruction from partially resolved gene trees. *BMC Bioinformatics*  
460 19, 15–30 (2018).

461 49. Chifman, J. & Kubatko, L. Quartet Inference from SNP Data Under the Coalescent  
462 Model. *Bioinformatics* 30, 3317–3324 (2014).

463 50. Malinsky, M., Matschiner, M. & Svardal, H. Dsuite - Fast D-statistics and related  
464 admixture evidence from VCF files. *Mol Ecol Resour* 21, 584–595 (2021).

465 51. Li, H. *et al.* The Sequence Alignment/Map format and SAMtools. *Bioinformatics* 25,  
466 2078–2079 (2009).

467 52. Helwig, N. Multiple and Generalized Nonparametric Regression. *SAGE Research*  
468 *Methods Foundations* Preprint at <https://doi.org/10.4135/9781526421036885885>  
469 (2020).

470 53. Pickrell, J. K. & Pritchard, J. K. Inference of Population Splits and Mixtures from  
471 Genome-Wide Allele Frequency Data. *PLoS Genet* 8, e1002967 (2012).

472 54. Wen, D., Yu, Y., Zhu, J. & Nakhleh, L. Inferring Phylogenetic Networks Using  
473 PhyloNet. *Syst Biol* 67, 735–740 (2018).

474 55. Pease, J. B. & Hahn, M. W. Detection and Polarization of Introgression in a Five-  
475 Taxon Phylogeny. *Syst Biol* 64, 651–662 (2015).

476 56. Fan, Z. *et al.* A multi-omics framework reveals strawberry flavor genes and their  
477 regulatory elements. *New Phytologist* (2022) doi:10.1111/NPH.18416.

478 57. Mao, J. *et al.* High-quality haplotype-resolved genome assembly of cultivated  
479 octoploid strawberry. *Hortic Res* 10, (2023).

480 58. Kokot, M., Dlugosz, M. & Deorowicz, S. KMC 3: counting and manipulating k-mer  
481 statistics. *Bioinformatics* 33, 2759–2761 (2017).

482 59. Langmead, B., Trapnell, C., Pop, M. & Salzberg, S. L. Ultrafast and memory-  
483 efficient alignment of short DNA sequences to the human genome. *Genome Biol*  
484 10, 1–10 (2009).

485 60. Ou, S. *et al.* Benchmarking transposable element annotation methods for creation  
486 of a streamlined, comprehensive pipeline. *Genome Biol* 20, 275 (2019).

487 61. Emms, D. M. & Kelly, S. OrthoFinder: Phylogenetic orthology inference for  
488 comparative genomics. *Genome Biol* 20, 1–14 (2019).

489 62. Katoh, K. & Standley, D. M. MAFFT Multiple Sequence Alignment Software Version  
490 7: Improvements in Performance and Usability. *Mol Biol Evol* 30, 772 (2013).

491 63. Sanderson, M. J. r8s: inferring absolute rates of molecular evolution  
492 and divergence times in the absence of a molecular clock. *Bioinformatics* 19, 301–  
493 302 (2003).

494 64. To, T. H., Jung, M., Lycett, S. & Gascuel, O. Fast Dating Using Least-Squares  
495 Criteria and Algorithms. *Syst Biol* 65, 82–97 (2016).

496 65. Tamura, K., Tao, Q. & Kumar, S. Theoretical Foundation of the RelTime Method for  
497 Estimating Divergence Times from Variable Evolutionary Rates. *Mol Biol Evol* 35,  
498 1770–1782 (2018).

499 66. Edelman, D. W. *The Eocene Germer Basin Flora of South-Central Idaho*. (1975).

500 67. Becker & F., H. The York Ranch Flora of the Upper Ruby Basin, Southwestern  
501 Montana. *Palaeontographica Abteilung B* 18–93 (1973).

502